Impact of different metakaolin mixtures on oligomer formation and geopolymer properties: Impurity effect

W.C. N'Cho, A. Gharzouni, Jenny Jouin, S. Rossignol

Open Ceramics 15 (2023) 100411

Contents lists available at ScienceDirect

Open Ceramics

journal homepage: www.sciencedirect.com/journal/open-ceramics

Impact of different metakaolin mixtures on oligomer formation and geopolymer properties: Impurity effect

W.C. N'cho [a], A. Gharzouni [a], J. Jouin [a], S. Rossignol [a,*]

[a] IRCER: Institute for Research on Ceramics (UMR CNRS 7315), European Center for Ceramics, 12 Rue Atlantis, Cedex, 87068, Limoges, France

ARTICLE INFO

Handling editor: P Colombo

Keywords:
Geopolymer
Aluminosilicate mixture
Viscosity
FTIR
Network
Oligomer formation

ABSTRACT

The impact of metakaolin mixtures on geopolymer formation and corresponding properties was evaluated by synthesizing geopolymers from mixtures of different metakaolins and 5 M potassium silicate. Mixture reactivity was investigated by viscosity, thermogravimetric (DTA-TGA), and in situ infrared spectroscopy (FTIR) measurements. Furthermore, mechanical strength and porosity measurements were undertaken on consolidated materials. The results have shown that the aluminum molar concentration governs the setting time and oligomer formation energy. Indeed, the high aluminum content associated with the high purity of the metakaolins lead to a low formation energy of oligomer, whereas for the metakaolins containing more impurities, the energy required for oligomer formation was higher. Regardless of the formulation, the mechanical strength and porosity trends were similar. Network characteristics were assessed by amorphous material content and in situ infrared spectroscopy (FTIR) analysis. It was demonstrated that (i) for Si/Al < 1.5, an amorphous network is formed with a constant Si/Al ratio, and for (ii) Si/Al > 1.5, different networks are formed. The zeta potential values of the different metakaolin mixtures corroborated these findings. Zeta potential values of metakaolins are governed by the impurities present in the metakaolins, which limit the release of aluminous species from the metakaolins in solution, emphasizing that knowledge of raw materials is essential to understand the local networks formation.

1. Introduction

Geopolymers are three-dimensional amorphous Si–O–Al materials obtained by the activation of an alkali silicate solution or an acid solution (orthophosphoric acid) with an aluminosilicate source (clays, metakaolins and industrial byproducts, etc.) at room temperature [1–3]. Geopolymers can develop interesting properties depending on the reactivity of the raw materials [4]. Reactivity studies of aluminosilicate sources have shown that metakaolins with a Si/Al ratio of 1 remain the most promising for the formation of geopolymer networks [5].

Different geological origins, thermal treatment processes (flash calcination, rotary furnace calcination) and impurity contents can modify the reactivity of metakaolins [6,7] and consequently impact geopolymer properties [8–11]. With so many different sources of metakaolins containing different impurities, few works have focused on the monitoring of geopolymerization mechanisms (from the fresh state to consolidation), in particular by considering the different stages of the reaction (dissolution of metakaolins, oligomer formation and polycondensation). To elucidate the role of metakaolin impurities in reaction mixtures, particularly their role in controlling the nature of formed networks, geopolymer properties were evaluated.

For commercial metakaolins, most of the work carried out on geopolymers has focused on an evaluation of fresh state properties, which have been highlighted by viscosity measurements, particularly in the presence of additives to regulate setting times for various applications (coatings, waste immobilization, grout formulations) [12–15]. Furthermore, differential calorimetry, infrared spectroscopy (FTIR) and in situ thermal analysis measurements were performed to monitor the kinetics of geopolymerization reactions and to evaluate network formation [4,10,16]. Moreover, the high reactivity of metakaolin has led to a particular interest in the evaluation of geopolymer working properties (mechanical strength) as well as microstructure [9,17,18]. In fact, it has been demonstrated that impurities such as quartz or anatase are not altered in alkaline medium and consequently they play a role as reinfort leading to different mechanical properties [19]. M. Nodehi et al. [20] suggested that quartz sand smaller than 1.18 mm, used as an inert filler, can be added to metakaolin-based geopolymers for the production of ultrahigh-performance geopolymer concrete with improved mechanical

* Corresponding author.
E-mail address: sylvie.rossignol@unilim.fr (S. Rossignol).

https://doi.org/10.1016/j.oceram.2023.100411
Received 13 June 2023; Received in revised form 12 July 2023; Accepted 13 July 2023
Available online 24 July 2023

properties. Similar conclusions were reached by P. Kathirvel et al. [21]. At the same time, it has been shown that the nature of the (Si/Al) networks of geopolymers is governed by the high reactivity of the alkaline solution [22]. Stevenson et al. [17] showed that the concentration of alkali ions and silicon led to lower porosity and a denser microstructure linked to better metakaolin dissolution. Moreover, an alkaline potassium solution leads to geopolymers with nanopore sizes and higher pore numbers compared to geopolymers based on sodium solution [23–25]. These results have led to a special interest in the geopolymerization mechanisms of different metakaolin mixtures, which is necessary to understand the role of metakaolin impurities in the reaction mixtures as well as their impact on geopolymer properties.

In a previous work [26], an evaluation of the reactivity of different metakaolin mixtures revealed that the physicochemical properties (specific surface, particle size) depended on the different initial metakaolins. Similarly, the structural properties (reactive aluminum and amorphous content determined by NMR spectroscopy and X-ray diffraction, respectively) were linked to the reference metakaolins. However, the zeta potential values did not seem to be related to the mixture ratios. The mineralogy, particularly the amount of silica-based impurities present, limited the zeta potential values to the lowest absolute value. The purpose of this study is to evaluate the influence of these different characteristics of metakaolin blends on geopolymer properties. The geopolymerization reactions were followed from the fresh state to the consolidated state by different physicochemical (viscosity measurements, thermal analysis) and structural (FTIR spectroscopy, amorphous content) characterization techniques. After consolidation, working properties such as compressive strength were evaluated, and porosity measurements were conducted. These steps were taken to predict the properties of the metakaolin mixtures.

2. Experimental part

2.1. Raw materials and sample preparation

Three aluminosilicate sources were chosen for this work and are listed in Table 1. Metakaolin M5 was supplied by Argeco (Fumel, France), while metakaolin M1 and kaolinite KI were provided by Imerys (Clerac, France). Before use, KI was calcined in a rotary furnace at 750 °C for 1 h 30 min with a heating and cooling rate of 5 °C.min^{-1}, resulting in the metakaolin denoted MI [26]. Potassium silicate solution S1 Geosil® 32,434 ([K] = 5 M, Si/M = 0.8) provided by Woellner was used [27]. The three metakaolins were mixed from an equimolar aluminum ternary diagram and mixed for 30 min at 45 tr/min using a Turbula® mixer. Finally, geopolymer samples were synthetized using the silicate solution and were consolidated at room temperature under endogenous conditions. To simplify the sample description, the different geopolymers were named Gi, G1, G5 for the pastes from the basic metakaolins MI, M1 and M5 respectively and Gi1, G15, Gi5, Gi15 for the samples based on the mixture of metakaolins MIM1, M1M5 MIM5 and MIM1M5 respectively.

2.2. Characterization

Viscosity measurements were carried out on fresh pastes cylindrical polystyrene vessels (Ø = 28.00 mm) with a rotational Brookfield Viscometer DV2T coupled with a low shear, low viscosity cylindrical spindle LV-04 (64) while varying the rotational speed, starting at 100 rpm (for viscosity up to 6 Pa s) and ending at 1 rpm (up to 1000 Pa s). Data were obtained by performing a test every 30 min. Between tests, pastes were kept sealed in cylindrical vessels and continuously stirred with a roller mixer to keep the pastes homogenized. Viscosity analysis allowed us to determine the initial viscosity η0 and the time of setting, which is the duration of time from paste reaction to consolidation [14].

Infrared spectroscopy measurements were performed on a Thermo-Fisher Scientific Nicolet 380 in ATR (Attenuated Total Reflectance) mode. Acquisitions were made between 4000 and 500 cm^{-1} every 10 min for 12 h with 64 scans with a resolution of 4 cm^{-1}. OMNIC software (Nicolet Instrument) was used to acquire and process the data. The evolution of bonds within the material is described by the superposition of the 72 spectra obtained. Thus, it is possible to plot the evolution of the Si–O-M band position (M = Si or Al), translating the substitution of Si–O–Si bonds by Si–O–Al bonds in the geopolymer matrix [28].

Differential thermal analysis (DTA) and thermogravimetric analysis (TGA) were performed on an SDTQ600 apparatus from TA Instruments in an atmosphere of dry flowing air (100 mL/min) in platinum crucibles. The signals were measured with Pt/Pt–10 %Rh thermocouples. Thermal analysis was conducted during the formation of the consolidated materials using a thermal cycle previously established by Autef et al. [29]. The fresh reactive mixtures were maintained at 70 °C for 2 h. Analysis of the heat flux and its derivative allowed for the identification of all the samples properties and the delineation of four zones during the consolidation that could be attributed to the different stages of the geopolymerization process. Additionally, the mass losses of the consolidated geopolymer materials were measured to identify and quantify water loss or decomposition in the samples.

Mercury intrusion porosimetry tests (MIP) were carried out using a Micromeritics Autopore IV 9510 porosimeter capable of detecting pore diameters between 3 nm and 360 μm at a mercury intrusion and extrusion volume of 0.1 μL. The mercury pressure was gradually increased from 0.0007 to 413.6854 MPa. The geopolymer sample was first placed in an oven at 50 °C for 12 h to eliminate any water that could prevent the intrusion of mercury into the porous network [30]. Then, the tests were performed in two steps. First, a low-pressure step was used to remove gases, fill the samples with mercury and perform the test with a pressure of 345 KPa. Then, a high-pressure step was performed with a pressure as high as 414 MPa [31].

Uniaxial compression tests were performed on cylindrical samples with an aspect ratio of 2 (Ø = 15 mm, h = 30 mm) after 7 days at room temperature. Instron 5969, with a load cell of 50 kN and a crosshead speed of 0.5 mm/min, was used. The reported maximum compressive strength σmax represents the average of seven samples.

The acquisition of diffractograms was performed on powder geopolymer samples with a Brucker-AXS D8 equipped with a copper anode (CuKα = 1.5418 Å) from 5° to 60° (2θ) with a step size of 0.02° and an equivalent acquisition time of 57 s. The crystalline phases were identified by comparison to ICDD (International Center for Diffraction) reference PDF (Powder Diffraction File).

Table 1
Nomenclature and composition of the different raw materials.

Name	Provider	Weight composition (%)		Heating process/Concentration
M5	ARGECO	SiO_2: 59.9	Al_2O_3: 35.3	Flash
M1	IMERYS	SiO_2: 55.0	Al_2O_3: 40.0	Rotary furnace
KI		SiO_2: 54	Al_2O_3: 46	

3. Results

3.1. Fresh state of geopolymers

3.1.1. Viscosity

The evolution of the different geopolymer paste viscosities over time is presented in Fig. 1. The initial viscosities and setting time values are reported in Table 2. The initial viscosities (η0) vary from 4 to 25 Pa s. The Gi, G1 and G5 samples display viscosity values of 4.2, 6.9 and 4.9 Pa s depending on the metakaolin used. Gi5 has a viscosity of 4.6 Pa s, a value between those of the Gi and G5 geopolymers. The other paste mixtures show higher viscosity values, especially Gi1 and Gi15, with values of 13.7 and 24.6 Pa s, respectively. The initial viscosity values of the geopolymer pastes from the metakaolin blends are independent of the geopolymers but linked to the metakaolin bases [27]. Regardless of

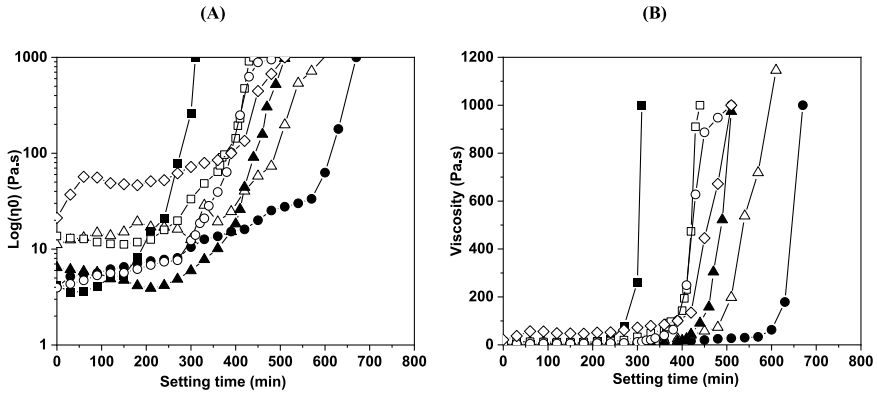

Fig. 1. (A) Initial viscosity and (B) viscosity value as a function of time for (●) Gi, (▲) G1, (■) G5, (□) G15, (○) Gi5, (Δ) Gi1, and (◊) Gi15) fresh mixture.

Table 2
Values of geopolymers in the fresh state: viscosity (η_0, setting time), Fourier transform infrared spectroscopy in situ (shift, slope), and thermal analysis (formation of oligomer energy).

Samples	η_0± 0.5 (Pa.s)	Setting time± 20 (min)	Shift± 4 (cm^{-1})	Slope± 0.002 (cm^{-1}/min)	Energy± 0.02(KJ.mol^{-1})	Time ±0.1 (min)
Gi	4.2	620	10	0.018	1.56	7.60
G1	6.9	430	14	0.026	1.8	7.60
G5	4.9	260	17	0.04	2.05	7.33
G15	12.7	380	16	0.027	1.91	7.58
Gi5	4.6	440	15	0.023	1.78	7.46
Gi1	13.7	510	8	0.022	1.95	7.60
Gi15	24.6	430	13	0.025	1.77	7.48

the geopolymer paste, the viscosity curves show two steps: first a stabilization step and then an exponential increase in viscosity characterizing the setting time [14]. Gi has the longest setting time (620 min). The other formulations from the mixtures involving metakaolin M5 and MI show fairly similar setting times of approximately 430 min. G5 (260 min) has a much shorter setting time. The long setting time of the Gi paste is related to the large amount of aluminous species dissolved for polycondensation. In fact, it has been shown in previous works that an increase in setting time is directly related to the amount of aluminum species present [32]. For pastes involving M5 metakaolin, the effect of M5 metakaolin is more pronounced due to impurities such as high quantities of quartz [26]. The setting time of the Gi1 paste (510 min) is higher than that of the other pastes involving metakaolin mixtures due to the small amount of impurities present in metakaolin M1. Thus, the effect of M1 metakaolin is low in the Gi1 paste. Finally, the setting time is mainly controlled by the raw materials. The behavior of the different geopolymer pastes over time allowed us to highlight the impact of the purity of the metakaolins, especially the concentration of aluminum in the mixtures. A correlation was established between the setting times of the geopolymers and the aluminum concentration of the different mixtures (Fig. 2). Regardless of the geopolymer paste, the setting times increase with the aluminum concentration of the geopolymers. The Gi geopolymer, which contains more aluminum ([Al] = 2.5 M) results in a longer setting time. In fact, Gi is sourced from a high-purity metakaolin, which increases the dissolution kinetics of reactive metakaolin species (aluminous and siliceous species) in the presence of alkali silicate solution. Thus, a high concentration of aluminum favors the trapping of water within the structure during polycondensation, increasing the setting time. In contrast to Gi, G5 (containing impurities such as quartz) has a shorter setting time and a low an aluminum concentration, which results in the slow formation of oligomers and facilitates the removal of water from the structure. Furthermore, it seems that the presence of impurities partially inhibits the release of aluminous species for the formation of oligomers [33].

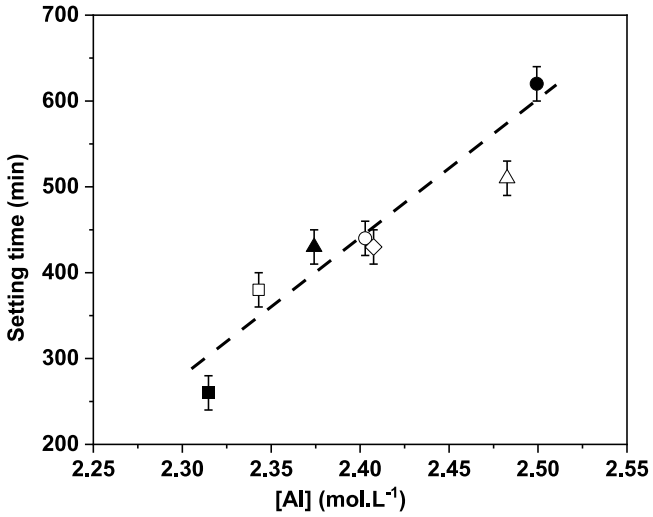

Fig. 2. Trends in setting times for (●) Gi, (▲) G1, (■) G5, (□) G15, (○) Gi5, (Δ) Gi1, and (◊) Gi15) fresh mixtures as a function of aluminum concentration.

3.1.2. Oligomer formation

To understand all these differences, Fourier transform infrared (FTIR) spectroscopy and in situ thermogravimetric analysis (DTA-TGA) were carried out to follow geopolymerization. The evolution of the Si–O-M (Q^2) bond position around 1000 cm^{-1} [34] in the spectra of the Gi, G5 and Gi5 pastes at t = 0 and t = 12 h is given in Fig. 3. The Gi sample shows a large peak at 3400 cm^{-1} at the beginning (t = 0 h), which is associated with the stretching of –OH, and a peak centered at 1630 cm^{-1} related to the bending of OH in water molecules [35]. Additionally, the weak vibrational band intensities at approximately 1425 cm^{-1} are characteristic of the stretching of O–C–O bonds [36]. Furthermore, an intense and large peak at approximately 1000 cm^{-1} corresponds to Si–O–M (Q^2) bonds (M = Si, Al) [34]. However, there is a noticeable transformation in these vibrational bands over time (t = 12 h). All the other geopolymer pastes show the same vibrational bands with identical behavior over time (provided in the supplementary file). Fig. 3B presents the evolution of the main peak linked to Si–O–M (Q^2) in Gi, G5 and Gi5. For the Gi sample, the initial position of Si–O–M (Q^2) is located at approximately 991 cm^{-1}, and the wavenumber decreases as a function of time. This variation indicates the substitution of Si–O–Si by Si–O–Al due to the polycondensation reaction [37]. The different shifts are 10, 15, and 17 cm^{-1} for the Gi, Gi5 and G5 samples with slopes of 0.018, 0.023 and 0.04 cm^{-1}, respectively (Table 2). Gi shows a small shift value

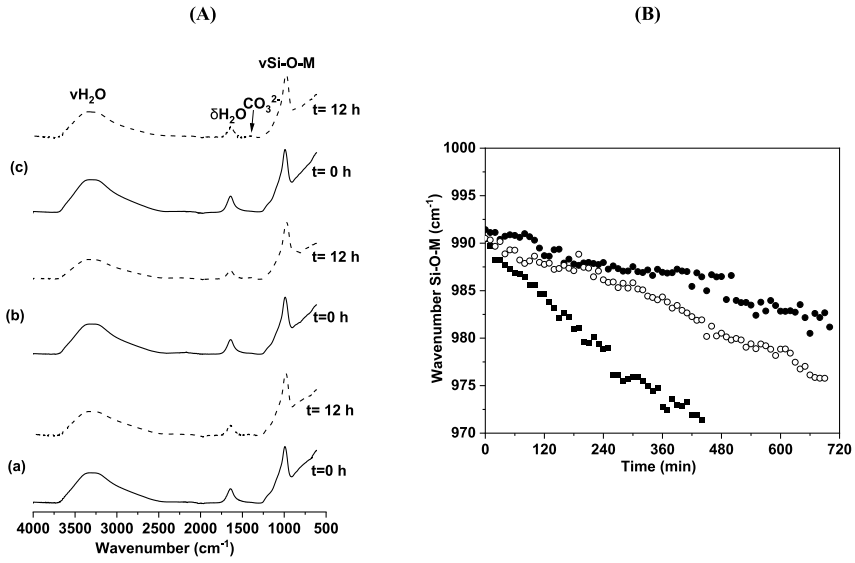

Fig. 3. (A) FTIR spectra of (A) Gi(a), G5(b), and Gi5(c) fresh mixture (t = 0, t = 12 h) and (B) evolution of the Si–*O*-M (Q^2) position over time for the (●) Gi, (■) G5), and (○) Gi5 geopolymer pastes.

associated with a small slope compared to sample G5, which has the highest shift value and a high slope. These observations reveal that the formation of a geopolymer network is more favored in Gi, which has faster substitution kinetics for the Si–O–Si bond with the Si–O–Al bond, while G5 shows the formation of different networks associated with slower substitution kinetics. The Gi5 mixture exhibits shift and slope values between those of the reference geopolymers; however, the shift value is closer to that of G5, which reveals the formation of a different network. In fact, Gi has the ability to more rapidly release the aluminum species necessary for the polycondensation reaction [33,38]. For G5 and Gi5, the release of metakaolin reactive species is low. The values obtained for the mixtures of metakaolins are between those of the basic metakaolins.

The geopolymerization reaction of the different pastes was also followed by thermal analysis at 70 °C. Fig. 4 shows a typical example of the heat flux and mass loss curves obtained for the Gi sample. According to previous work [29], zone I is associated with the reorganization of species, zone II is characteristic of the dissolution of metakaolin, zone III is attributed to the formation of oligomers, and zone IV is attributed to polycondensation. The same observations were made for the other geopolymers, as shown in the supplementary file. From the heat flow curves, the values of the energies and formation times of the oligomers were determined and reported in Table 2. Regardless of the geopolymer, the values of the energies of formation of oligomers vary between 1.56 and 2.05 kJ mol^{-1}, which is associated with a polycondensation time from 7.60 to 7.33 min as a function of the geopolymer paste type. Gi sample has the lowest energy (1.56 kJ mol^{-1}) and longer formation times (7.60 min), reflecting the availability of a large quantity of dissolved reactive alumina species necessary for the formation of oligomers [25]. The G5 geopolymer has the highest energy (2.05 kJ mol^{-1}) and a shorter formation time (7.33 min), suggesting a limited quantity of dissolved species and the presence of impurities in the metakaolin. For the geopolymers from the metakaolin mixtures, the energy values are between those of the basic metakaolins, especially the pastes from metakaolins involving metakaolin M5, G15 (1.91 kJ mol^{-1}), Gi5 (1.78 kJ mol^{-1}), Gi15 (1.77 kJ mol^{-1}), which have shorter oligomer formation times of 7.58, 7.46, and 7.48 min, respectively. In the case of pure metakaolin, the aluminous species react rapidly. However, with impurities the dissolution is delayed due to impurities. These differences in energies are related to the behavior of metakaolins to react in presence of impurities in alkaline medium, as a result, more energy is required for oligomer formation [39].

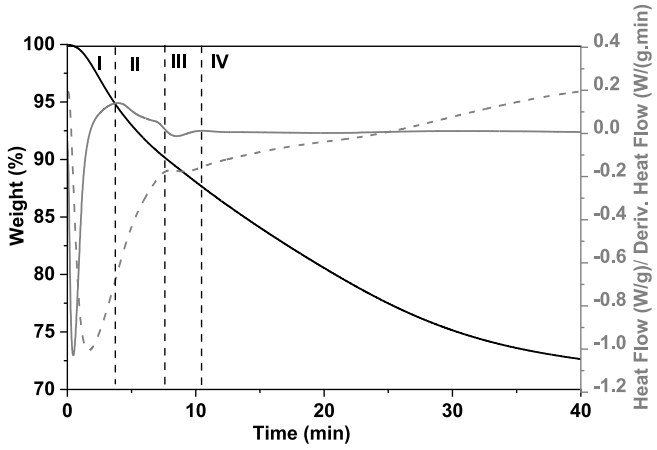

Fig. 4. In situ geopolymer Gi formation based on thermal analysis at 70 °C as a function of time.

All these data evidence that two behaviors can be distinguished. Metakaolins without impurities show small shifts (more substitution of Al for Si), low energies of oligomer formation and longer setting times. In contrast, metakaolins containing impurities have larger shifts, require more energy to form oligomers and have shorter setting times. The values characterizing the different geopolymer pastes from the metakaolin mixtures are between those of the reference geopolymers.

3.2. Consolidated state

The different behaviors of the geopolymer pastes were highlighted, mechanical properties (porosity, compressive strength) were analyzed, and structural analysis was conducted to ascertain the amorphous material content of the consolidated geopolymers and their water content.

3.2.1. Porosity

Porosity measurements conducted by mercury intrusion on selected geopolymer (Gi, G5 and Gi5) samples allowed for the determination of the open porosity rate and the pore size distribution (Fig. 5). Information

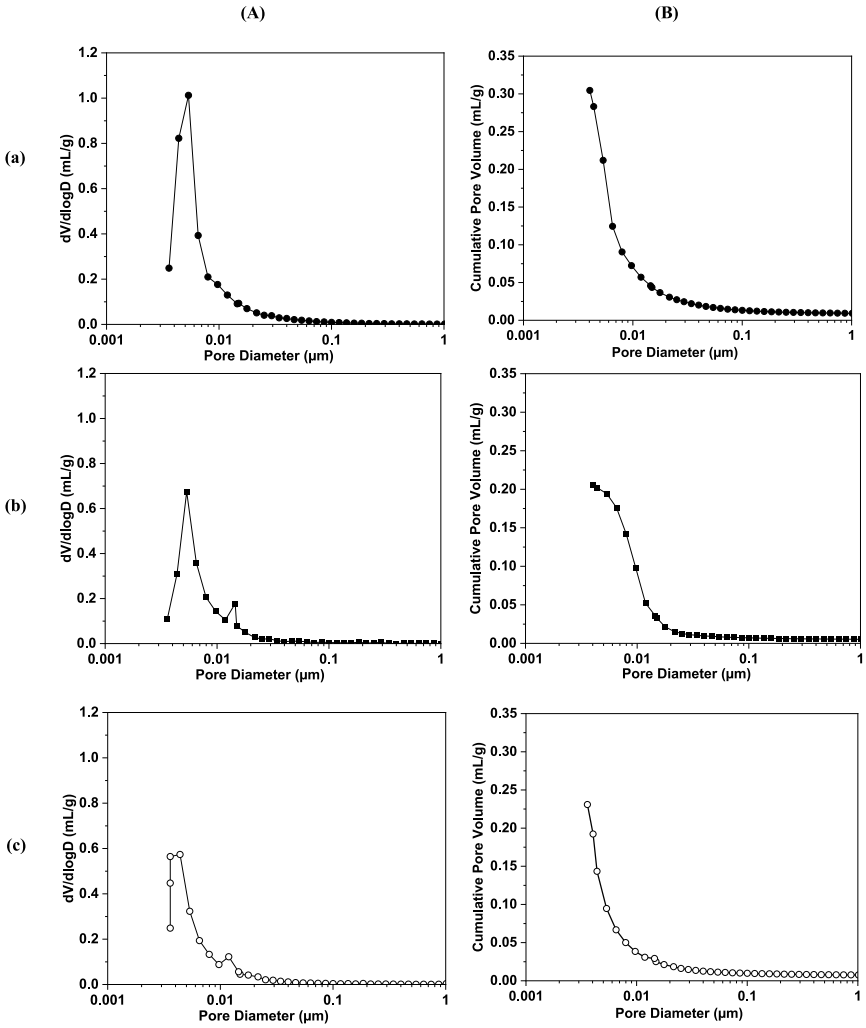

Fig. 5. (A) Evolution of the volume derivative of mercury intrusion and (B) cumulative pore volume as a function of (●) Gi (a), (■) G5 (b), and (○) Gi5 (c) geopolymer pore size.

on the other geopolymers can be seen in the supplementary file. Regardless of the geopolymer, the porosity values vary between 30 and 40%, with nanopores centered mainly at approximately 5 nm. These behaviors are in agreement with the works of Scanferla et al., [27]. Gi exhibits a unimodal pore size distribution with a total porosity of 40%. G5 displays a total porosity of 30% with a bimodal distribution with small pore sizes of 5 nm and large pore sizes of approximately 0.015 μm based on the different networks formed, which is related to the amount of quartz present in the M5 metakaolin [26]. The same behavior is observed for Gi5, which is centered around two pore sizes (approximately 5 nm and 0.015 μm) and has a total porosity of 33%. The same observations were made for the other geopolymers involving mixtures of metakaolins, which present heterogeneous networks due to the presence of impurities. The different porosity values of the G15, Gi1 and Gi15 geopolymers are 32, 34 and 31%, respectively. These values are between those of the reference geopolymers. Furthermore, the porosity of the different geopolymers varies little, except for Gi, which is more porous and homogeneous due to the high purity of the MI metakaolin.

3.2.2. *Mechanical performance*

Mechanical tests were performed on the different consolidated geopolymer materials after 7 days of storage under endogenous conditions. All values of the geopolymer samples are reported in Table 3. Regardless of the geopolymer, the results of the mechanical tests vary little (between 55 and 65 MPa), as presented in Table 3. The Gi geopolymer shows a mechanical strength of 55 MPa. However, G5 yields a slightly higher value of 65 MPa due to the presence of silica in the M5 metakaolin, which favors granular stacking that acts as reinforcement [40, 41]. Samples G15, Gi5, Gi1 and Gi15 display the same value of approximately 58 MPa based on the solution used regardless of the metakaolin source. The water contents deduced from thermal analysis are reported in Table 3. The values vary between 20 and 28% depending on the geopolymer. The GI geopolymer shows the highest amount of 28%, and the sample G5 geopolymer displays the lowest value of 20%, in agreement with the mechanical resistance values obtained. Additionally, Gi5 exhibits a value of 23% between the Gi and G5 values. These differences can be explained by the oligomer formation energies.

Table 3
Values of geopolymers in the consolidated state: porosity measurements, compressive strength, water content (DTA-TGA), amorphous rate (XRD).

Samples	Porosity ±1 (%)	Σ± 3 (MPa)	Water content± 1 (%)	Amorphous± 1 (%)
Gi	40	55	28	99
G1	33	60	24	70
G5	30	65	20	58
G15	32	58	21	64
Gi5	33	57	23	79
Gi1	34	60	27	85
Gi15	31	58	22	75

In fact, geopolymers with pure metakaolin display fast oligomer formation, and some water is trapped in the nanopores [33]. In contrast, geopolymers involving metakaolins with impurities show different oligomers, resulting in less water being trapped in the network [33].

3.2.3. Mineralogical characterization

The structural data of the consolidated geopolymers highlighted by X-ray diffraction confirm these results. In fact, the diffractogram of Gi shows the presence of a large amorphous dome, whereas the diffractograms of the G5 and Gi5 mixtures are mainly composed of crystallized phases from undissolved impurities and several small amorphous domes (Fig. 6). The same observations were made for the other geopolymers involving metakaolins M1 and M5, as shown in the supplementary file. Furthermore, the amorphous content of the different geopolymers was evaluated. The results are reported in Table 3. The amorphous material content values vary between 58 and 99%. The Gi geopolymers have the highest amorphous material content (99%) within a geopolymer network, and the G5 geopolymers present the lowest amorphous material content (58%), which explains the formation of different networks. The values obtained for the Gi5 geopolymers (79%) are between those of Gi and G5. The same observation was made for the other geopolymers involving metakaolin mixtures.

4. Discussion

The formation of the different networks can be demonstrated by the magnitude and direction of shifts and by slope values deduced from FTIR analysis as a function of the amorphous geopolymer material content (Fig. 7). The shifts (values of Q^2) and slope show different behaviors as a function of the amorphous material content. The shifts show a linear and decreasing trend from low amorphous material content (presence of impurities) to the highest corresponding to the pure metakaolins (Si/Al = 1). The slope variation displays an exponential decrease and tends to plateau for amorphous content values > 70% for pure metakaolin (Si/Al = 1). These observations show that the presence of impurities in the metakaolins induces high slope values and leads to the formation of different networks. All these observations agree with the work of Gharzouni et al. [11] and Autef et al. [42] which revealed that impurities in metakaolins are responsible for the formation of several networks.

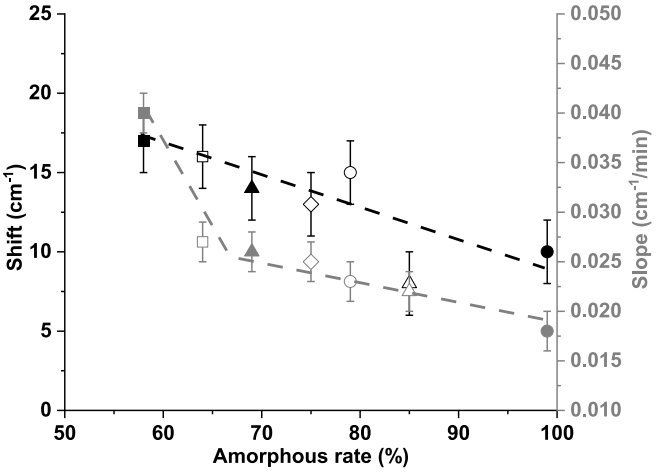

Fig. 7. Value of the Q^2 shift (– – – –) and slope (– – – –) as a function of amorphous material content of (●) Gi, (▲) G1, (■) G5, (□) G15, (○) Gi5, (Δ) Gi1, and (◊) Gi15) geopolymers as determined by XRD.

Fig. 8 shows the geopolymer mechanical data, water content, amorphous material content and zeta potential values of metakaolins [26] as a function of the geopolymer Si/Al molar ratio to establish correlations between the reactivity of the raw materials and the features of the geopolymer binders. These data underline that the mechanical values in this case are strongly dependent on the silicate solution used. Indeed, in previous work, it has been demonstrated the reactivity of alkaline solution governs the geopolymers mechanical properties [25]. Furthermore, as mentioned by Gunasekara et al. a slow increase in the compressive strength value with the zeta potential value can be noticed [43]. For the data related to the networks resulting from polycondensation reactions, the variations show two behaviors. For a value of Si/Al < 1.5, there is a dissolution of the species in the alkaline solution and therefore the formation of the same kind of oligomer, leading to a network of the same chemical composition [11,42] and an amorphous material content of almost 100%. For Si/Al ratios >1.5, particularly high Si/Al values (1.7), the water content and amorphous material content are lower due to the formation of different oligomer types, leading to

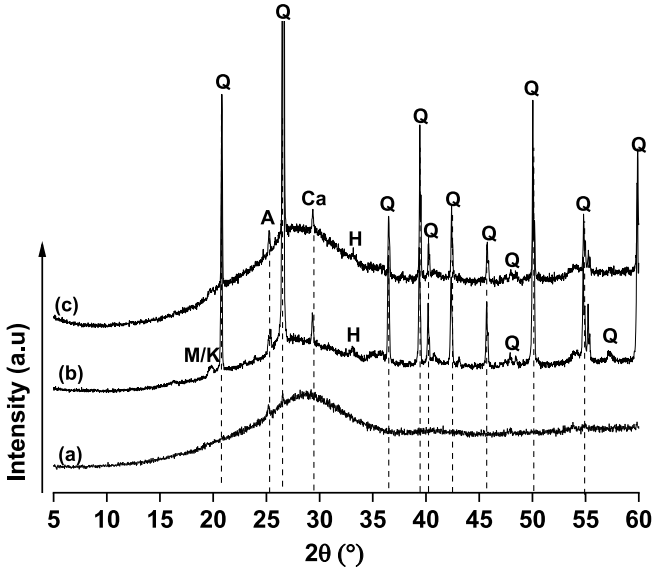

Fig. 6. Diffractograms of (a) Gi, (b) G5, and (c) Gi5 geopolymers (PDF file: Q: quartz (01-083-2465), M: muscovite (00-003-0849), K: kaolinite (00-012-0447), A: anatase (01-071-1166), Ca: calcite (00-005-0586), H: hematite (01-079-1741)).

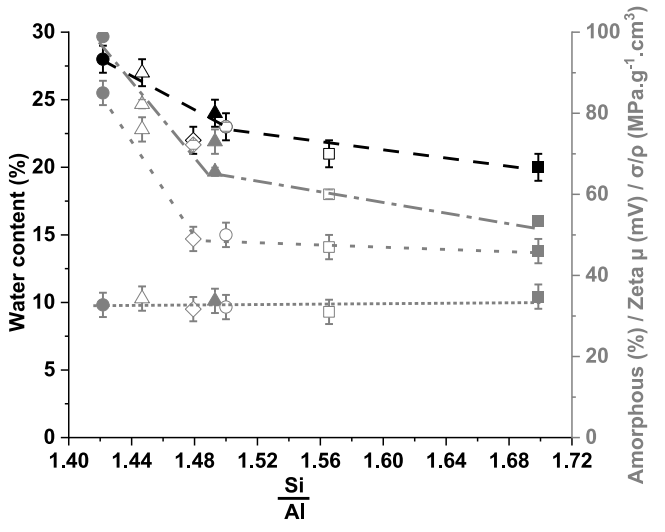

Fig. 8. Trends in (– – – – –) water content, (– · – · –) amorphous material content, (– – – – –) metakaolin zeta potential and (·····) compressive strength as a function of $\frac{Si}{Al}$ for (●) Gi, (▲) G1, (■) G5, (□) G15, (○) Gi5, (Δ) Gi1, and (◊) Gi15) geopolymers.

different polycondensation reactions and therefore to different networks linked to the metakaolin impurities. This behavior is similar to the variation in the zeta potential of metakaolins as a function of the Si/Al ratio. Indeed, in previous works [26], it was demonstrated that the reactivity of different metakaolin mixtures involves different zeta potential values depending on the mineralogy of the metakaolin used. In fact, at pH = 11, the zeta potential value was lower for pure metakaolins (−85 mV) than for metakaolins containing impurities (approximately −50 mV) [26]. Consequently, these variations observed for both amorphous and water contents of the same order as the zeta potential suggest that it is possible to predict geopolymer properties as a function of zeta potential values.

5. Conclusion

This study was conducted to understand the effects of different metakaolin mixtures with the same aluminum content on their reactions with a reactive alkaline solution. The geopolymerization reaction was followed in the fresh state by several physicochemical and structural characterization techniques, and then mechanical properties were evaluated. The viscosity measurements showed that setting times increased with the purity of the metakaolin and the molar concentration of aluminum. In situ thermal analysis revealed a low energy requirement for oligomer formation for geopolymers with pure metakaolins compared to metakaolins containing impurities. The mechanical properties of the consolidated materials, as evidenced by compressive strength and porosity measurements, were almost identical regardless of the geopolymer. The local order determined by the amorphous material content based on in situ infrared spectroscopy (FTIR) measurements can be expressed as follows:

- For Si/Al < 1.5, there is amorphous network formation (constant Si/Al).
- for Si/Al > 1.5, different networks are formed (different Si/Al).

Finally, the zeta potential values of the different metakaolin mixtures corroborate these data collected on a local scale, allowing us to predict some behaviors. Based on the results of this work, the impact of these different properties on shaping will be studied.

Declaration of competing interest

The authors declare that they have no known competing financial interests or personal relationships that could have appeared to influence the work reported in this paper.

Appendix A. Supplementary data

Supplementary data to this article can be found online at https://doi.org/10.1016/j.oceram.2023.100411.

References

[1] J. Davidovits, Chemistry and Applications, second ed., Geopolymer Institute, Saint Quentin, France, 2008.
[2] G. Barone, C. Finocchiaro, I. Lancellotti, C. Leonelli, P. Mazzoleni, C. Sgarlata, A. Stroscio, Potentiality of the use of pyroclastic volcanic residues in the production of alkali activated, Material Waste and Biomass Valorization 12 (2021) 1075–1094.
[3] H. Celerier, J. Jouin, V. Mathivet, N. Tessier-Doyen, S. Rossignol, Composition and properties of phosphoric acid–based geopolymers, J. Non-Cryst. Solids 493 (2018) 94–98.
[4] A. Gharzouni, I. Sobrados, E. Joussein, S. Baklouti, S. Rossignol, Control of polycondensation reaction generated from different metakaolins and alkaline solutions, J. Ceram. Sci. Technol. 8 (3) (2017) 365–376.
[5] Y.J. Zhang, S. Li, Y.C. Wang, D.L. Xu, Microstructural and strength evolutions of geopolymer composite reinforced by resin exposed to elevated temperature, J. Non-Cryst. Solids 358 (2012) 620–624.
[6] F. Zibouche, H. Kerdjoudj, J.B. d'Espinose de Lacaillerie, H. VanDamme, Geopolymers from Algerian metakaolin. Influence of secondary minerals, Appl. Clay Sci. 43 (2009) 453–458.
[7] A. Elimbi, K.H. Tchakoute, D. Njopwouo, Effects of calcination temperature of kaolinite clays on the properties of geopolymer cements, Construct. Build. Mater. 25 (2011) 2805–2812.
[8] L. Atmaja, H. Fansuri, A. Maharani, Crystalline phase reactivity in the synthesis of fly ash–based geopolymer, Indo. J. Chem. 11 (2011) 90–95.
[9] Qian Wan, Feng Rao, Shaoxian Song, F. Diana, Cholico-González, Noemí L. Ortiz, Combination formation in the reinforcement of metakaolin geopolymers with quartz sand, Cement Concr, Compos 80 (2017) 115–122.
[10] A. Autef, E. Joussein, A. Poulesquen, G. Gasgnier, S. Pronier, I. Sobrados, J. Sanz, S. Rossignol, Influence of metakaolin purities on potassium geopolymer formulation: the existence of several networks, J. Colloid Interface Sci. 408 (2013) 43–53.
[11] A. Gharzouni, E. Joussein, S. Baklouti, S. Pronier, I. Sobrados, J. Sanz, S. Rossignol, The effect of an activation solution with siliceous species on the chemical reactivity and mechanical properties of geopolymers, J. of Sol-Gel Sci. (2014) article in press.
[12] Z. Zhang, H. Wang, Alkali-activated Cements for Protective Coating of OPC Concrete Handbook of Alkali-Activated Cements, Mortars and Concretes, Woodhead Publishing, Oxford, 2015, pp. 605–626.
[13] I. Lancellotti, M. Catauro, C. Ponzoni, F. Bollino, C. Leonelli, Inorganic polymers from alkali activation of metakaolin: effect of setting and curing on structure, J. Solid State Chem. 200 (2013) 341–348.
[14] C. Dupuy, A. Gharzouni, I. Sobrados, N. Tessier-Doyen, N. Texier-Mandoki, X. Bourbon, S. Rossignol, Formulation of an alkali-activated grout based on Callovo-Oxfordian argillite for an application in geological radioactive waste disposal, Construct. Build. Mater. 232 (2020) 117–170.
[15] Archez, N. Texier-Mandoki, X. Bourbon, J.F. Caron, S. Rossignol, Influence of the wollastonite and glass fibers on geopolymer composites workability and mechanical properties, Construct. Build. Mater. 257 (2020), 119511.
[16] G. Liang, W. Yao, A. She, New insights into the early-age reaction kinetics of metakaolin geopolymer by 1H low-field NMR and isothermal calorimetry, Cement Concr. Compos. 137 (March 2023), 104932.
[17] M. Stevenson, K. Sagoe-Crentsil, Relationships between composition, structure and strength of inorganic polymers, J. Mater. Sci. 40 (2005) 2023–2036.
[18] E. Kamseu, V. Catania, C. Djangang, V.M. Sglavo, C. Leonelli, Correlation between microstructural evolution and mechanical properties of a-quartz and alumina reinforced K-geopolymers during high temperature treatments, Adv. Appl. Ceram. 111 (3) (2012) 120–128.
[19] E. Autef, Joussein, A. Poulesquen, G. Gasgnier, S. Pronier, I. Sobrados, Role of metakaolin dehydroxylation in geopolymer synthesis, Powder Technol. 250 (2013) 33–39.
[20] M. Nodehi, Aguayo Federico, Ultra high performance and high strength geopolymer concrete, J. of Build. Pathology. Rehabilitation. 6 (1) (2021) 34.
[21] P. Kathirvel, S. Sreenath, Sustainable development of ultrahigh-performance concrete using geopolymer technology, J. Build. Eng. 39 (2021). Article 102267.
[22] L. Vidal, A. Gharzouni, S. Rossignol, Alkaline silicate solutions: an overview of their structure, reactivity and applications, in: The Handbook of Sol'Gel Science and Technology, second ed., 2016, pp. 181–204.
[23] J.L. Bell, W.M. Kriven, M. Gordon, Microstructure and nanoporosity of as-set geopolymers, mechanical properties and performance of engineering ceramics II, Ceram. Eng. Sci. Proc. 27 (2006) 491–503.
[24] J.L. Bell, W.M. Kriven, Nanoporosity in aluminosilicate, geopolymeric cements, Microsc. Microanal. 10 (2004) 590–591.
[25] A. Gharzouni, E. Joussein, B. Samet, S. Baklouti, S. Rossignol, Effect of the reactivity of alkaline solution and metakaolin on geopolymer formation, J. Non-Cryst. Solids 410 (2014) 127–134, 2015.
[26] W. N'cho, A. Gharzouni, J. Jouin, A. Aimable, I. Sobrados, S. Rossignol, Effect of mixing metakaolins: methodological approach to estimate metakaolin reactivity, Ceram. Int. 49 (2023) 20334–20342.
[27] P. Scanferla, A. Gharzouni, N. Texier-Mandoki, X. Bourbon, S. Rossignol, Effects of potassium-silicate, sands and carbonates concentrations on metakaolin-based geopolymers for high-temperature applications, Open Ceramics 10 (2022), 100257.
[28] E. Prud'homme, P. Michaud, E. Joussein, J.M. Clacens, S. Rossignol, Role of alkaline cations and water content on geomaterial foams: monitoring during formation, J. Non-Cryst. Solids 357 (2011) 1270–1278.
[29] A. Autef, E. Joussein, G. Gasgnier, S. Rossignol, Role of the silica source on the geopolymerization rate: a thermal analysis study, J. Non-Cryst. Solids 366 (2013) 13–21.
[30] C. Gallé, Effect of drying on cement-based materials pore structure as identified by mercury intrusion porosimetry: a comparative study between oven-, vacuum-, and freeze-drying, Cement Concr. Res. 31 (Issue 10) (October 2001) 1467–1477.
[31] Z. Peng, K. Vance, A. Dakhane, R. Marzke, N. Neithalath, Microstructural and 29Si MAS NMR spectroscopic evaluations of alkali cationic effects on fly ash activation, Cement Concr. Compos. 57 (2015) 34–43.
[32] A. Gharzouni, L. Vidal, N. Essaidi, E. Joussein, S. Rossignol, Recycling, of geopolymer waste: influence on geopolymer formation and mechanical properties, Mater. Des. 94 (2016) 221–229.
[33] A. Autef, E. Joussein, A. Poulesquen, G. Gasgnier, S. Pronier, I. Sobrados, J. Sanz, S. Rossignol, Influence of metakaolin purities on potassium geopolymer formulation: the existence of several networks, J. Colloid Interface Sci. 408 (2013) 43–53.
[34] C. Dupuy, A. Gharzouni, N. Texier-Mandoki, X. Bourbon, S. Rossignol, Alkali-Activated materials based on callovo-oxfordian argillite: formation, structure and mechanical properties, J. Ceram. Sci. Technol. 9 (2) (2018) 127–140.

[35] J. Archez, N. Texier-Mandoki, X. Bourbon, J.F. Caron, S. Rossignol, Influence of the wollastonite and glass fibers on geopolymer composites workability and mechanical properties, Construct. Build. Mater. 257 (2020), 119511.
[36] I.G. Lodeiro, D.E. Macphee, A. Palomo A. Fernandez-Jimenez, Effect of alkalis on fresh C–S-H gels. FTIR analysis, Cement Concr. Res. 39 (3) (2009) 147–153.
[37] A. Gharzouni, B. Samet, S. Baklouti, E. Joussein, S. Rossignol, Addition of low reactive clay into metakaolin-based geopolymer formulation: synthesis, existence domains and properties, Powder Technol. 288 (2016) 212–220.
[38] V. Medri, S. Fabbri, J. Dedecek, Z. Sobalik, Z. Tvaruzkova, A. Vaccari, Role of the morphology and the dehydroxylation of metakaolins on geopolymerization, Appl. Clay Sci. 50 (2010) 538–545.
[39] A. Fernandez-Jimenez, A.G. de la Torre, A. Palomo, G. Lopez-Olmo, M.M. Alonso, M.A.G. Aranda, Quantitative determination of phases in the alkaline activation of fly ash, PartII: Degree of reaction, Fuel 85 (2006) 1960–1969.
[40] H. Celerier, J. Jouin, V. Mathivet, N. Tessier-Doyen, S. Rossignol, Composition and properties of phosphoric acid–based geopolymers, J. Non-Cryst. Solids 493 (2018) 94–98.
[41] V. Mathivet, Géopolymère en milieu acide : compréhension du processus réactionnel et développement de composites thèse de doctorat université de Limoges, 2021.
[42] L. Weng, K. Sagoe-Crentsil, Dissolution processes, hydrolysis and condensation reactions during geopolymer synthesis: Part I-Low Si/Al ratio systems, J. Mater. Sci. 42 (9) (2007) 2997–3006.
[43] C. Gunasekara, D.W. Law, S. Setunge, J.G. Sanjayan, Zeta potential, gel formation and compressive strength of low calcium fly ash geopolymers, Construct. Build. Mater. 95 (2015) 592–599.